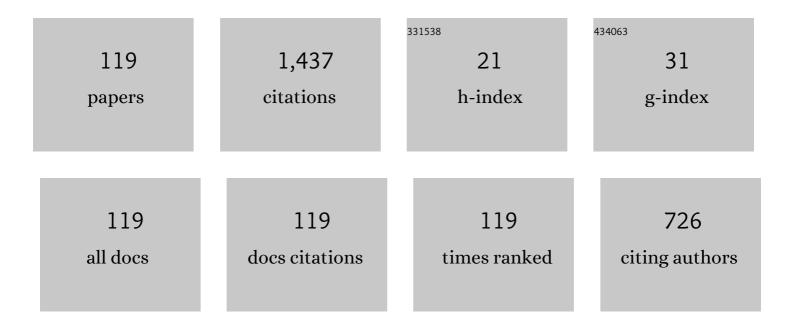
## List of Publications by Year in descending order

Source: https://exaly.com/author-pdf/11238261/publications.pdf Version: 2024-02-01



| #  | Article  | IF  | CITATIONS |
|----|--|-----|-----------|
| 1  | Design of a large-range rotary microgripper with freeform geometries using a genetic algorithm.<br>Microsystems and Nanoengineering, 2022, 8, 3.   | 3.4 | 10        |
| 2  | Correlated Theory of Cross-Axis Interference of MEMS Devices Based on Parallel Plate and Squeeze<br>Film Air Damping Induced Suppression. IEEE Sensors Journal, 2022, 22, 6698-6705.                                       | 2.4 | 0         |
| 3  | A Mems Electro-Mechanical Co-Optimization Platform Featuring Freeform Geometry Optimization<br>Based on a Genetic Algorithm. , 2022, , .   |     | О         |
| 4  | High-performance panoramic annular lens design for real-time semantic segmentation on aerial imagery. Optical Engineering, 2022, 61, .   | 0.5 | 5         |
| 5  | Accurate mechanical–optical theoretical model of cross-axis sensitivity of an interferometric micro-optomechanical accelerometer. Applied Optics, 2022, 61, 3201.  | 0.9 | Ο         |
| 6  | Design of stereo imaging system with a panoramic annular lens and a convex mirror. Optics Express, 2022, 30, 19017.  | 1.7 | 8         |
| 7  | Semi-analytic Fresnel diffraction calculation with polynomial decomposition. Optics Letters, 2022, 47, 3776.   | 1.7 | 2         |
| 8  | Analysis and correction of spherical aberrations in long focal length measurements. Optics Communications, 2021, 482, 126564.  | 1.0 | 3         |
| 9  | Hierarchical visual localization for visually impaired people using multimodal images. Expert Systems<br>With Applications, 2021, 165, 113743.   | 4.4 | 13        |
| 10 | Genetic Algorithm for the Design of Freeform Geometries in a Large-Range Rotary Microgripper. , 2021, , .  |     | 1         |
| 11 | A Mems Accelerometer with an Auto-Tuning System Based on an Electrostatic Anti-Spring. , 2021, , .   |     | 4         |
| 12 | Feature-based characterization and extraction of ripple errors over the large square aperture. Optics<br>Express, 2021, 29, 8296.  | 1.7 | 5         |
| 13 | Corrections to "Design, Optimization, and Realization of a High Performance MOEMS Accelerometer<br>From a Double-Device-Layer SOI Wafer―[Aug 17 859-869]. Journal of Microelectromechanical Systems,<br>2021, 30, 331-331. | 1.7 | ο         |
| 14 | Non-propagation fast phase diverse phase retrieval for wavefront measurement with generalized FFT-based basis function. Optics Express, 2021, 29, 18817.   | 1.7 | 0         |
| 15 | Investigation of the Influence of Temperature and Humidity on the Bandwidth of an Accelerometer.<br>Micromachines, 2021, 12, 860.  | 1.4 | 1         |
| 16 | Panoramic annular SLAM with loop closure and global optimization. Applied Optics, 2021, 60, 6264.  | 0.9 | 18        |
| 17 | Design of a compact varifocal panoramic system based on the mechanical zoom method. Applied Optics, 2021, 60, 6448.  | 0.9 | 14        |
| 18 | Investigation of a complete squeeze-film damping model for MEMS devices. Microsystems and Nanoengineering, 2021, 7, 54.  | 3.4 | 17        |

| #  | Article   | IF  | CITATIONS |
|----|---|-----|-----------|
| 19 | Cross-iteration multi-step optimization strategy for three-dimensional intensity position correction in phase diverse phase retrieval. Optics Express, 2021, 29, 29186.             | 1.7 | 2         |
| 20 | Two characterization methods of ripple errors for the large square aperture. Applied Optics, 2021, 60, 8706.  | 0.9 | 0         |
| 21 | Large-scale phase retrieval method for wavefront reconstruction with multi-stage random phase modulation. Optics Communications, 2021, 498, 127115.                                 | 1.0 | 5         |
| 22 | A Temperature Control Method for Microaccelerometer Chips Based on Genetic Algorithm and Fuzzy<br>PID Control. Micromachines, 2021, 12, 1511.                                       | 1.4 | 6         |
| 23 | Interferometric measurement of freeform surfaces using irregular subaperture stitching.<br>Measurement Science and Technology, 2020, 31, 055202.                                    | 1.4 | 6         |
| 24 | Optimum wavelength of spaceborne oceanic lidar in penetration depth. Journal of Quantitative Spectroscopy and Radiative Transfer, 2020, 256, 107310.                                | 1.1 | 9         |
| 25 | Micromachined Accelerometers with Sub-µg/â^šHz Noise Floor: A Review. Sensors, 2020, 20, 4054.  | 2.1 | 56        |
| 26 | A Semianalytic Monte Carlo Simulator for Spaceborne Oceanic Lidar: Framework and Preliminary<br>Results. Remote Sensing, 2020, 12, 2820.  | 1.8 | 11        |
| 27 | Design of freeform geometries in a MEMS accelerometer with a mechanical motion preamplifier based on a genetic algorithm. Microsystems and Nanoengineering, 2020, 6, 104.           | 3.4 | 12        |
| 28 | Comparison of Fiber-to-Waveguide Couplers in Point Diffraction Interferometer Based on Waveguide<br>Reference Wavefront Source. Applied Sciences (Switzerland), 2020, 10, 9115.     | 1.3 | 0         |
| 29 | Investigation of the thermal deformation of a chip-scale packaged optical accelerometer.<br>Measurement: Journal of the International Measurement Confederation, 2020, 163, 108017. | 2.5 | 4         |
| 30 | Accurate phase retrieval algorithm based on linear correlation in self-calibration phase-shifting interferometry with blind phase shifts. Optics Communications, 2020, 466, 125612. | 1.0 | 6         |
| 31 | Unifying Visual Localization and Scene Recognition for People With Visual Impairment. IEEE Access, 2020, 8, 64284-64296.  | 2.6 | 16        |
| 32 | Dual-view catadioptric panoramic system based on even aspheric elements. Applied Optics, 2020, 59,<br>7630.   | 0.9 | 12        |
| 33 | Simultaneous reconstruction of phase and amplitude for wavefront measurements based on nonlinear optimization algorithms. Optics Express, 2020, 28, 19726.                          | 1.7 | 8         |
| 34 | Modal-based nonlinear optimization algorithm for wavefront measurement with under-sampled data.<br>Optics Letters, 2020, 45, 5456.  | 1.7 | 7         |
| 35 | Non-null testing of the aspheric surface using a quadriwave lateral shearing interferometer. Applied Optics, 2020, 59, 5447.  | 0.9 | 3         |
| 36 | OpenMPR: Recognize places using multimodal data for people with visual impairments. Measurement<br>Science and Technology, 2019, 30, 124004.  | 1.4 | 9         |

| #  | Article   | IF  | CITATIONS |
|----|---|-----|-----------|
| 37 | Genetic Algorithm for the Design of Freeform Geometries in a MEMS Accelerometer Comprising a<br>Mechanical Motion Pre-Amplifier. , 2019, , .  |     | 4         |
| 38 | A semianalytic Monte Carlo radiative transfer model for polarized oceanic lidar: Experiment-based<br>comparisons and multiple scattering effects analyses. Journal of Quantitative Spectroscopy and<br>Radiative Transfer, 2019, 237, 106638. | 1.1 | 21        |
| 39 | Panoramic Annular Localizer: Tackling the Variation Challenges of Outdoor Localization Using<br>Panoramic Annular Images and Active Deep Descriptors. , 2019, , .   |     | 18        |
| 40 | Misalignment correction for free-form surface in non-null interferometric testing. Optics Communications, 2019, 437, 204-213.   | 1.0 | 6         |
| 41 | Assisting the visually impaired: multitarget warning through millimeter wave radar and RGB-depth sensors. Journal of Electronic Imaging, 2019, 28, 1.   | 0.5 | 16        |
| 42 | Representation of complex optical surfaces with adaptive radial basis functions. Applied Optics, 2019, 58, 3938.  | 0.9 | 3         |
| 43 | PALVO: visual odometry based on panoramic annular lens. Optics Express, 2019, 27, 24481.  | 1.7 | 17        |
| 44 | Real-time pedestrian crossing lights detection algorithm for the visually impaired. Multimedia Tools and Applications, 2018, 77, 20651-20671.   | 2.6 | 26        |
| 45 | Optical vortex beam direct-writing photolithography. Applied Physics Express, 2018, 11, 036503.   | 1.1 | 7         |
| 46 | Long-Range Traversability Awareness and Low-Lying Obstacle Negotiation with RealSense for the Visually Impaired. , 2018, , .  |     | 15        |
| 47 | Optical Acceleration Measurement Method with Large Non-ambiguity Range and High Resolution via<br>Synthetic Wavelength and Single Wavelength Superheterodyne Interferometry. Sensors, 2018, 18, 3417.   | 2.1 | 2         |
| 48 | Reducing the minimum range of a RGB-depth sensor to aid navigation in visually impaired individuals.<br>Applied Optics, 2018, 57, 2809.   | 0.9 | 14        |
| 49 | Characterization of the pinhole diffraction based on the waveguide effect in a point diffraction interferometer. Applied Optics, 2018, 57, 781.   | 0.9 | 4         |
| 50 | Single Chip-Based Nano-Optomechanical Accelerometer Based on Subwavelength Grating Pair and Rotated Serpentine Springs. Sensors, 2018, 18, 2036.  | 2.1 | 15        |
| 51 | Comprehensive design and calibration of an even aspheric quarter-wave plate for polarization point diffraction interferometry. Applied Optics, 2018, 57, 1789.  | 0.9 | 5         |
| 52 | Fusion of millimeter wave radar and RGB-depth sensors for assisted navigation of the visually impaired. , 2018, , .   |     | 6         |
| 53 | Relationship between the effective attenuation coefficient of spaceborne lidar signal and the IOPs of seawater. Optics Express, 2018, 26, 30278.  | 1.7 | 19        |
| 54 | 3D simulation for scatter light distribution of optical surface defects. , 2018, , .  |     | 1         |

| #  | Article  | IF  | CITATIONS |
|----|--|-----|-----------|
| 55 | A pressure-tuned field-widened Michelson interferometer system as the spectroscopic filter of high-spectral-resolution lidar. , 2018, , .  |     | 0         |
| 56 | Thermal stress of MOEMS accelerometers based on grating interferometric cavity. , 2018, , .  |     | 0         |
| 57 | Design, Optimization, and Realization of a High-Performance MOEMS Accelerometer From a<br>Double-Device-Layer SOI Wafer. Journal of Microelectromechanical Systems, 2017, 26, 859-869. | 1.7 | 41        |
| 58 | Surface defects evaluation system based on electromagnetic model simulation and inverse-recognition calibration method. Optics Communications, 2017, 390, 88-98.                       | 1.0 | 12        |
| 59 | Determination of thermally induced effects and design guidelines of optomechanical accelerometers.<br>Measurement Science and Technology, 2017, 28, 115201.                            | 1.4 | 5         |
| 60 | Practical retrace error correction in non-null aspheric testing: A comparison. Optics Communications, 2017, 383, 378-385.  | 1.0 | 17        |
| 61 | IR stereo RealSense: Decreasing minimum range of navigational assistance for visually impaired individuals. Journal of Ambient Intelligence and Smart Environments, 2017, 9, 743-755.  | 0.8 | 20        |
| 62 | Design of the closed-loop capacitive microaccelerometer based on PSpice. , 2017, , .   |     | 2         |
| 63 | Polarization properties of receiving telescopes in atmospheric remote sensing polarization lidars.<br>Applied Optics, 2017, 56, 6837.  | 0.9 | 12        |
| 64 | Design of iodine absorption cell for high-spectral-resolution lidar. Optics Express, 2017, 25, 15913.  | 1.7 | 27        |
| 65 | Generalized high-spectral-resolution lidar technique with a multimode laser for aerosol remote sensing. Optics Express, 2017, 25, 979.   | 1.7 | 10        |
| 66 | Target enhanced 3D reconstruction based on polarization-coded structured light. Optics Express, 2017, 25, 1173.  | 1.7 | 48        |
| 67 | Retrieving the seawater volume scattering function at the 180° scattering angle with a high-spectral-resolution lidar. Optics Express, 2017, 25, 11813.                                | 1.7 | 15        |
| 68 | Compact polarization-based dual-view panoramic lens. Applied Optics, 2017, 56, 6283.   | 0.9 | 11        |
| 69 | Polarimetric target depth sensing in ambient illumination based on polarization-coded structured light. Applied Optics, 2017, 56, 7741.  | 0.9 | 13        |
| 70 | Detecting Traversable Area and Water Hazards for the Visually Impaired with a pRGB-D Sensor.<br>Sensors, 2017, 17, 1890.   | 2.1 | 34        |
| 71 | Spherical aberration compensation method for long focal-length measurement based on Talbot interferometry. Proceedings of SPIE, 2017, , .  | 0.8 | 0         |
| 72 | Expanding the Detection of Traversable Area with RealSense for the Visually Impaired. Sensors, 2016, 16, 1954.   | 2.1 | 73        |

| #  | Article  | IF  | CITATIONS |
|----|--|-----|-----------|
| 73 | Design of the interferometric spectral discrimination filters for a three-wavelength high-spectral-resolution lidar. Optics Express, 2016, 24, 27622.                  | 1.7 | 5         |
| 74 | The analysis of temperature effect and temperature compensation of MOEMS accelerometer based on a grating interferometric cavity. Proceedings of SPIE, 2016, , .       | 0.8 | 3         |
| 75 | Design of a panoramic long-wave infrared athermal system. Optical Engineering, 2016, 55, 125103.   | 0.5 | 2         |
| 76 | High-spectral-resolution lidar for ocean biological carbon pump studies. , 2016, , .   |     | 1         |
| 77 | Field-widened Michelson interferometer for spectral discrimination in high-spectral-resolution lidar: practical development. Optics Express, 2016, 24, 7232.           | 1.7 | 13        |
| 78 | Polarized high-spectral-resolution lidar based on field-widened Michelson interferometer.<br>Proceedings of SPIE, 2016, , .  | 0.8 | 1         |
| 79 | Comprehensive view of high-spectral-resolution lidar technique from the perspective of spectral discrimination. Proceedings of SPIE, 2016, , .                         | 0.8 | 0         |
| 80 | Comparison of two panoramic front unit arrangements in design of a super wide angle panoramic annular lens. Applied Optics, 2016, 55, 3219.                            | 0.9 | 20        |
| 81 | Mechanical design optimization of a single-axis MOEMS accelerometer based on a grating interferometry cavity for ultrahigh sensitivity. Proceedings of SPIE, 2016, , . | 0.8 | 2         |
| 82 | Frequency locking of a field-widened Michelson interferometer based on optimal multi-harmonics heterodyning. Optics Letters, 2016, 41, 3916.                           | 1.7 | 7         |
| 83 | Non-blind area PAL system design based on dichroic filter. Optics Express, 2016, 24, 4913.   | 1.7 | 17        |
| 84 | A novel design of dual-channel optical system of star-tracker based on non-blind area PAL system. ,<br>2016, , .   |     | 0         |
| 85 | Full-aperture long focal-length measurement based on divergent beam. Journal of Physics: Conference<br>Series, 2016, 680, 012012.                                      | 0.3 | 1         |
| 86 | Minimizing cross-axis sensitivity in grating-based optomechanical accelerometers. Optics Express, 2016, 24, 9094.  | 1.7 | 40        |
| 87 | Field-widened Michelson interferometer system as the spectroscopic filter of high-spectral-resolution lidar. , 2016, , .   |     | 0         |
| 88 | High-spectral-resolution lidar for ocean ecosystem studies. Proceedings of SPIE, 2016, , .   | 0.8 | 3         |
| 89 | Practical phase unwrapping of interferometric fringes based on unscented Kalman filter technique.<br>Optics Express, 2015, 23, 32337.                                  | 1.7 | 58        |
| 90 | Analysis of the imaging performance of panoramic annular lens with conic conformal dome. , 2015, , .   |     | 0         |

| #   | Article  | IF  | CITATIONS |
|-----|--|-----|-----------|
| 91  | Recent developments of interferometric wavefront sensing. , 2015, , .  |     | 0         |
| 92  | General measurement of optical system aberrations with a continuously variable lateral shear ratio by a randomly encoded hybrid grating. Applied Optics, 2015, 54, 8913. | 2.1 | 19        |
| 93  | Calibration method for high accuracy measurement of long focal length with Talbot interferometry:<br>reply. Applied Optics, 2015, 54, 10573.                             | 2.1 | 2         |
| 94  | Photolithography using lateral surface of nanofibers. Optics Communications, 2015, 343, 195-200.   | 1.0 | 1         |
| 95  | Subnanometer resolution displacement sensor based on a grating interferometric cavity with intensity compensation and phase modulation. Applied Optics, 2015, 54, 4188.  | 2.1 | 34        |
| 96  | Field-widened Michelson interferometer for spectral discrimination in high-spectral-resolution lidar: theoretical framework. Optics Express, 2015, 23, 12117.            | 1.7 | 27        |
| 97  | Aspheric subaperture stitching based on system modeling. Optics Express, 2015, 23, 19176.  | 1.7 | 28        |
| 98  | Quadriwave lateral shearing interferometer based on a randomly encoded hybrid grating. Optics<br>Letters, 2015, 40, 2245.  | 1.7 | 40        |
| 99  | Aberration calibration in high-NA spherical surfaces measurement on point diffraction interferometry. Applied Optics, 2015, 54, 3877.                                    | 2.1 | 12        |
| 100 | Tolerance analysis and optimization of a lateral deformable NEMS zeroth-order gratings. Optics<br>Communications, 2015, 355, 356-366.                                    | 1.0 | 4         |
| 101 | A MOEMS Accelerometer Based on Diffraction Grating with Improved Mechanical Structure.<br>International Journal of Automation Technology, 2015, 9, 473-481.              | 0.5 | 3         |
| 102 | Distortion control for panoramic annular lens with Q-type aspheres. Proceedings of SPIE, 2014, , .   | 0.8 | 0         |
| 103 | Focused laser lithographic system with sub-wavelength resolution based on vortex laser induced opacity of photochromic material. Optics Letters, 2014, 39, 6707.         | 1.7 | 5         |
| 104 | Long focal-length measurement using divergent beam and two gratings of different periods. Optics<br>Express, 2014, 22, 27921.  | 1.7 | 22        |
| 105 | Common-path and compact wavefront diagnosis system based on cross grating lateral shearing interferometer. Applied Optics, 2014, 53, 7144.                               | 0.9 | 24        |
| 106 | Design of vari-focal panoramic annular lenses based on Alvarez surfaces. , 2014, , .   |     | 6         |
| 107 | Stray light analysis and suppression of panoramic annular lens. Optics Express, 2013, 21, 10810.   | 1.7 | 23        |
| 108 | Design of panoramic stereo imaging with single optical system. Optics Express, 2012, 20, 6085.   | 1.7 | 32        |

| #   | Article  | IF  | CITATIONS |
|-----|--|-----|-----------|
| 109 | Calibration method for high-accuracy measurement of long focal length with Talbot interferometry.<br>Applied Optics, 2012, 51, 2407.                               | 0.9 | 24        |
| 110 | Optical accelerometer based on grating interferometer with phase modulation technique. Applied Optics, 2012, 51, 7005.   | 0.9 | 33        |
| 111 | A high-resolution displacement sensor based on a grating interferometer with the phase modulation technique. Measurement Science and Technology, 2012, 23, 105102. | 1.4 | 13        |
| 112 | Design of a panoramic annular lens with a horizontal symmetric FOV. Proceedings of SPIE, 2012, , .   | 0.8 | 1         |
| 113 | Nanometer-scale displacement sensor based on phase-sensitive diffraction grating. Applied Optics, 2011, 50, 1413.  | 2.1 | 33        |
| 114 | Parallel lensless optical correlator based on two phase-only spatial light modulators. Optics Express, 2011, 19, 12594.  | 1.7 | 5         |
| 115 | Compact optical correlator based on one phase-only spatial light modulator. Optics Letters, 2011, 36, 1383.  | 1.7 | 17        |
| 116 | An improved image restoration method for the high definition panoramic camera system. Optics and Lasers in Engineering, 2009, 47, 982-989.                         | 2.0 | 2         |
| 117 | Laser direct writing using submicron-diameter fibers. Optics Express, 2009, 17, 19960.   | 1.7 | 13        |
| 118 | Panoramic optical annular staring inspection system for evaluating the inner surface of a pipe. , 2007, ,  |     | 2         |
| 119 | Design of a nanoramic annular lens with a long focal length Applied Optics 2007 46, 7850   | 91  | 97        |